EPJ manuscript No.
(will be inserted by the editor)

Model simulations of ground-state and finite-temperature properties of disordered magnetic nanostructures

N. Douarche,[1] F. Calvo,[1] P. J. Jensen,[1,2] and G. M. Pastor[1]

[1]Laboratoire de Physique Quantique, Univertsité Paul Sabatier, CNRS, 31062 Toulouse, France
[2]Institut für Theoretische Physik, Freie Universität Berlin, Arnimallee 14, 14195 Berlin, Germany

Received: date / Revised version: date

Abstract. The properties of two-dimensional ensembles of magnetic nanoparticles that interact by magnetic dipole coupling are investigated. The low-temperature magnetic arrangements, the average binding energy $E_{\rm dip}$ due to dipolar interactions, and its scaling behavior with respect to the particle density C are calculated for different types of structural disorder and particle-size distribution. Many different metastable magnetic states are obtained, which exhibit strong noncollinearities and are reminiscent of a spin-glass behavior. For a given C, $|E_{\rm dip}|$ increases with increasing disorder of the particle positions. For random distributions at low particle densities $C \leq 0.2$, $E_{\rm dip}$ is dominated by the contributions of short interparticle distances. Thus, it scales as $|E_{\rm dip}| \propto C^{\alpha}$ with an unusually small exponent $\alpha = 0.85$–1. The straightforward scaling of the dipole interaction, $\alpha \simeq 3/2$, is obtained only for $C \geq 0.5$ or for nearly periodic ensembles. The finite temperature behavior of these disordered interacting nanomagnets is explored. The specific heat and magnetic susceptibility are calculated by performing Monte Carlo (MC) simulations. The onset of long-range magnetic order is discussed. In addition we determine hysteresis loops at finite temperatures and compare the results for different degrees of disorder.

PACS. PACS-key – PACS-key

1 Introduction

The properties of interacting magnetic nanostructured materials are currently the subject of a very intense research activity which is driven both by their fundamental interest and by the perspectives of technological applications [1]. Numerous experimental and theoretical studies have been performed on various two-dimensional (2D) and three-dimensional (3D) arrangements having different degrees of structural and magnetic disorder [2–4]. In these systems the magnetic particles are sufficiently small so that they usually stay in a single-domain magnetic state. Therefore, they can be viewed as giant classical magnetic moments (Stoner-Wohlfahrt particles). The magnetic behavior of nanostructure materials is conditioned by single-particle properties, such as lattice and shape anisotropies, and by interparticle interactions. The latter comprises the magnetic dipole coupling, the indirect exchange or Rudermann-Kittel-Kasuya-Yosida (RKKY) interaction mediated by the conduction electrons of a metal substrate, and the short-range direct exchange interaction in case of direct particle contact. The relative importance of these contributions can be tuned experimentally to some extent by changing the sample characteristics, like particle-size distribution, nanostructure morphology, or average interparticle distance. For low particle concentration C the interactions can be treated as a perturbation to the single-particle contributions. However, with increasing C the interparticle couplings tend to dominate and the single-particle approach is no longer applicable [3,4]. Therefore, in the most relevant case of large coverages, an explicit treatment of the interactions is crucial.

The nonuniform and competing nature of the magnetic couplings between the particles and the presence of significant disorder in the nanostructure (particle size- and shape dispersion, positional disorder, random anisotropy axes) result in a magnetic order which is similar to the one of a spin-glass system [5]. Consequently, many different metastable states exist, which are characterized by strong magnetic non-collinearities. Taking into account the complexity of this problem, it is of considerable interest to determine how the magnetic order or the interaction energy depends on sample parameters, particularly in the presence of disordered. Comparison between theory and experiment could then be used to infer the intrinsic microscopic parameters of the system and to optimize the sample characteristics for a given specific magnetic response.

From a fundamental standpoint, an intriguing open question is to understand to what extent the interactions may result in a collectively ordered magnetic state of such a disordered particle ensemble. For a dipole-coupled square layer, the ground state is the so-called columnar magnetic arrangement with a vanishing net magnetization, and the

parallel (ferromagnetic) alignment is a metastable state. Despite the fact that the dipole coupling itself is not rotationally invariant, the square layer exhibits a continuous rotational degeneracy for classical spins at $T = 0$. This accidental degeneracy is caused by the underlying symmetry of the lattice, and a small deviation from this symmetry lifts it. A long-range magnetic order is therefore not expected for a square layer at finite temperatures, due to the Mermin-Wagner theorem. However, as already shown by Monte Carlo studies and interacting spin-wave theory, a magnetic ordering with finite critical temperature does exist for dipole coupled spins on a square lattice, since the magnetic excitations are not continuously degenerate [6]. This behavior is an example of the 'order-by-disorder' effect in frustrated magnets [7]. Thermal fluctuations or lattice disturbances partly remove frustrations, and a collective magnetic ordering may emerge. On the other side, a random structural disorder or vacancies introduce easy axes along the lattice diagonals. Thus, the ordering effects of the dispersion of particle positions and the thermal agitations compete with each other. The magnetic binding energy and the magnetic arrangements are important to determine the long-range magnetic order and the critical temperature.

Several experiments on interacting high-density ferrofluid systems indicate the onset of a collectively ordered state below a characteristic concentration-dependent temperature [3]. Furthermore, recent measurements on Co islands deposited on Cu(001) exhibit a magnetic hysteresis and remanence in the temperature range up to $100K$ also for coverages below the magnetic percolation threshold [8]. These findings cannot be explained by single-particle blocking effects, due to the very small size of the Co islands. Notice that a precise experimental determination of the ordering temperature is a difficult task, since the relaxation times are often very long.

The purpose of this communication is to report on current simulations of ground-state and finite-temperature properties of 2D disordered magnetic nanostructures. In Sec. 2 the modelisation of the problem is briefly described. Results for low temperature properties like the average dipole energy per particle are presented and discussed in Sec. 3. Sec. 4 is concerned with the temperature dependence of magnetic susceptibilities and hysteresis loops and with the possible onset of long-range order. We conclude in Sec. 5 by pointing out some relevant extensions.

2 Model

The magnetic nanostructures are modeled by considering a 2D rectangular $L \times L$ unit cell with non-overlapping, disk- or sphere-shaped magnetic particles. An infinitely extended particle ensemble is obtained by imposing periodic boundary conditions. Alternatively, one may also consider open boundary conditions to realize a finite particle ensemble. Within the unit cell the particles can have different types of lateral arrangements: (i) a periodic square array, where the particle centers are located on the sites of a periodic lattice with lattice constant R_0, (ii) a disturbed or quasi-periodic array where the particle centers deviate from the square array following a Gaussian distribution $P(\mathbf{R})$ with a standard deviation σ_R, and (iii) a fully random distribution of particles within the unit cell. Since the direct exchange interaction between atomic magnetic moments is very strong, each particle i can be viewed as a single magnetic domain carrying a giant spin $M_i \sim N_i \mu_{at}$, where μ_{at} is the atomic magnetic moment. For simplicity, we restrict the moments to be confined to the xy-plane, their directions are then defined by azimuthal angles ϕ_i. The particle sizes N_i, i.e., the number of spins in each particle, are taken to be either the same for all particles, or dispersed around a mean value $\overline{N}$ following a Gaussian or a log-normal distribution with standard deviation σ_N.

The energy of a configuration of particle magnetic moments $\mathbf{M}_i$ is given by

$$\mathcal{H} = \frac{\mu_0}{2} \sum_{\substack{i,j \\ i \neq j}} \left[\mathbf{M}_i \cdot \mathbf{M}_j \, r_{ij}^2 - 3 \left(\mathbf{r}_{ij} \cdot \mathbf{M}_i \right) \left(\mathbf{r}_{ij} \cdot \mathbf{M}_j \right) \right] r_{ij}^{-5} - \mu_0 \sum_i \left(\mathbf{B} \cdot \mathbf{M}_i \right) . \quad (1)$$

The first term is the magnetic dipole interaction, where $r_{ij} = |\mathbf{r}_{ij}| = |\mathbf{r}_i - \mathbf{r}_j|$ is the distance between the centers of particles i and j, and μ_0 the vacuum permeability. The second term represents the Zeeman interaction with an external magnetic field $\mathbf{B}$, which enters in the calculation of the magnetic response and hysteresis loops.

The infinite range of the dipole interaction is taken into account by applying an Ewald-type summation over all periodically arranged unit cells of the extended thin film [9]. In addition to the usual point-dipole sum we consider the leading correction resulting from the dipole-quadrupole interaction. This so called area correction is of the order $(A_i + A_j)/r_{ij}^2$, with $A_i \propto N_i$ the area of particle i. For large particle coverages or small interparticle distances, it can amount to 50% of the point dipole sum. Note that this contribution vanishes for spherically shaped particles which have zero quadrupole moment. The atomic magnetic moment μ_{at}, given in Bohr magnetons μ_B, and the interatomic distance a_0 define the unit of dipole-coupling energy $w = \mu_{at}^2/a_0^3$. For example, values appropriate to Fe ($\mu_{at} = 2.2\mu_B$ and $a_0 = 2.5$ Å) yield $w = 0.19K$.

3 Low temperature properties

The low-temperature magnetic configurations and the average dipole energy per particle are determined as follows. Starting from an arbitrary initial guess $\{\phi_i^0\}$ of the magnetic directions, the total magnetic energy of the system is relaxed to the nearest local minimum by optimizing all the in-plane angles ϕ_i using a conjugated gradient method. In order to account for the many different local energy minima in case of disorder, the magnetic energy E is averaged over many different initial guesses for the same particle arrangement. In addition, many different realizations of the unit cell are considered, using the same global variables which characterize the particle ensemble (average

size, standard deviations, etc.). For the sake of comparison, E has been also calculated for a parallel magnetization ($\phi_i = \phi_p$ for all i). In this case E is averaged over all in-plane orientation ϕ_p. The magnetic energy is referred to the one of a random set of angles $\{\phi_i\}$ for which $E_{dip} = 0$.

The low temperature configurations of the magnetic moments are strongly non-collinear with small or vanishing net magnetization, a demagnetizing effect due to flux closure. The magnetic-energy landscape exhibits a probably very large number of local minima which have, for the most part, nearby energies and which are often separated by small energy barriers. Note that these non-collinear arrangements should not be considered as a disordered state, since the local magnetizations are strongly correlated by the dipole interaction.

The average magnetic dipole energy per island E_{dip} has been determined as a function of the standard deviation σ_r which characterizes the positional disorder. One observes that $|E_{dip}|$ increases with increasing disorder, reaching its maximum for a fully random setup of the island ensemble. The increase of $|E_{dip}|$ with respect to the uniform system amounts to roughly 50 %. In contrast, the island-size dispersion has no large effect on E_{dip}. The different trends for these two types of disorder can be understood by recalling that E_{dip} is a bilinear function of the island sizes N_i. Thus, the size-dispersion effect averages out for a symmetrical distribution of sizes around the mean value $\overline{N}$. On the other side, the dipole energy shows a nonlinear dependence on the interparticle distances: $E_{dip} \propto r_{ij}^{-3}$. Thus, with increasing positional disorder, the decrease of $|E_{dip}|$ for r_{ij} larger than average is more than counterbalanced by the increase of $|E_{dip}|$ coming from smaller values of r_{ij} between other pairs of islands. This leads to an increase of the average magnetic binding energy of the nanostructure and can be regarded as a first indication of order by disorder.

The contributions of short interparticle distances are also very important for the dependence of the magnetic energy on particle concentration C. As shown in Fig. 1, $E_{\rm dip}$ scales as $|E_{\rm dip}| \propto C^{\alpha}$ with an unusually small exponent $\alpha = 0.85$–1. This is very different from the straightforward scaling of the dipole interaction, $\alpha \simeq 3/2$, which is obtained only for $C \geq 0.5$ or for nearly periodic ensembles. For a parallel magnetic arrangement the effective exponent is $\alpha_p \simeq 1$, which is not very far from the result for relaxed arrangements. Therefore, part of the reduction of α, from 3/2 to 1, can be regarded as a dimensional effect which is nearly independent of the complex low-temperature magnetic order. Besides this, an additional reduction of α, from 1 to about 0.85, is a consequence of the noncollinear arrangement of the magnetic moments.

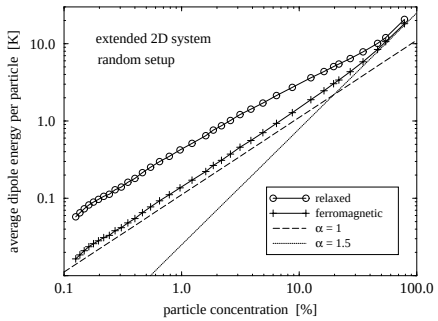

Fig. 1. Average dipole energy per particle E_{dip} of a 2D random ensemble of magnetic nanoparticles as a function of particle concentration C (logarithmic scale). Results are given for relaxed arrangements of magnetic moments and assuming a ferromagnetic alignment. Dashed (dotted) lines indicate the power-law behavior $E_{dip} \propto C^{\alpha}$ with $\alpha = 1$ ($\alpha = 3/2$).

4 Temperature dependent properties

The finite-temperature properties have been investigated by performing Metropolis Monte Carlo (MC) simulations. As discussed in the previous section, these systems are expected to show a spin-glass behavior, which is likely to result in a drastic slowing down of the convergence of conventional simulations. To overcome this problem of broken ergodicity, we have improved the MC method using a parallel tempering (PT) strategy [10,11]. The basic idea is to perform simultaneously all the simulations at the different temperatures $\{T_\alpha\}$, and to allow occasional exchanges between the configurations of MC trajectories corresponding to adjacent temperatures. At each step, with probability χ, the usual local Metropolis moves are performed for all trajectories. With probability $1 - \chi$, an exchange is attempted between a pair of randomly chosen adjacent trajectories having T_α and $T_\gamma = T_{\alpha+1}$. If we denote by $\mathcal{M}_\alpha$ and $\mathcal{M}_\gamma$ the corresponding initial configurations at these respective temperatures, then the probability for accepting the exchange between them is given by [11]

$$\mathrm{acc}(\mathcal{M}_\alpha \rightleftharpoons \mathcal{M}_\gamma) = \min\left[1, \exp(-\Delta\beta\Delta E)\right], \qquad (2)$$

where $\Delta\beta = 1/k_B T_\alpha - 1/k_B T_\gamma$ and $\Delta E = \mathcal{H}(\mathcal{M}_\alpha) - \mathcal{H}(\mathcal{M}_\gamma)$.

In addition to the PT algorithm, we have also implemented a more recent approach due to Wang and Landau (WL) [12]. This method consists in calculating iteratively, but directly, the microcanonical density of states by penalizing the statistical weight of each newly visited state. The WL algorithm has been shown to be particularly efficient for classical spin-glass systems [12]. The results reported here were obtained considering a set of 50 temperatures in the range $0 \leq T \leq 2$ K and performing 1.5×10^6 MC cycles for each trajectory, of which 5×10^5 cycles were discarded for equilibration.

Fig. 2 shows equilibrium properties of two magnetic nanostructure arrays with different degrees of disorder: no translational disorder and completely random location of the particles. The size-dispersion is weak and the same in both cases. All results have been averaged over 20 different realizations of disorder. From a computational point of view, one observes a very good agreement between the PT and WL methods. This is a good indication that our simulations have nearly converged. The peak in the heat capacity $C_V(T)$ of the weakly disordered system, and the

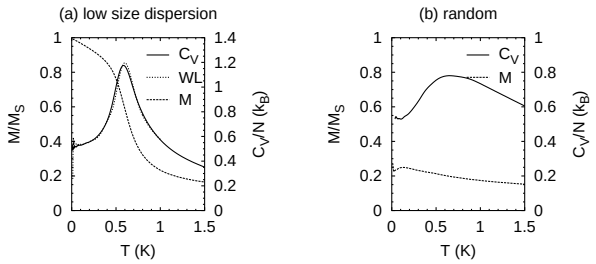

Fig. 2. Temperature dependence of the specific heat C_V and magnetization M of two-dimensional disordered nanostructures of small magnetic particles.

inflexion point in the temperature dependence of the magnetization $M(T)$, suggest the presence of a phase transition rounded by effect of the finite size L of the simulation cell. Indeed, more extended calculations as a function of L show a narrowing of the peak in $C_V(T)$ for increasing L. In case of important degree of disorder one observes a significant broadening of the peak in $C_V(T)$ and the disappearance of all structure in $M(T)$. Notice that for weak disorder and low temperatures (below the peak in C_V) the magnetization is maximum and that it rapidly drops at $T \sim 0.6$ K or by increasing disorder. This can be interpreted as the existence of a long-range-order phase which is destroyed by structural disorder and/or by temperature.

Typical magnetization curves $M(B)$ as a function of applied magnetic field B are displayed in Fig. 3. Two different degrees of size dispersion are considered without translational disorder. The step-like pattern in $M(B)$ suggests that the nanostructures have a very complex potential energy landscape. Small changes in the applied field can make the system jump from a potential well to another part of the landscape leading to sharp changes in the spin configuration and in M. This picture is also supported by the larger magnitude of the steps found upon increasing disorder. Again, the results indicate a spin-glass-like behavior of the magnetic nanostructures.

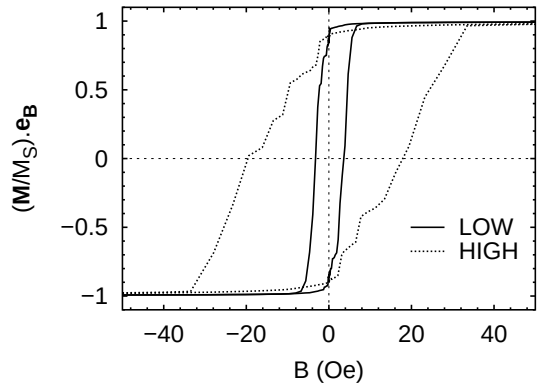

Fig. 3. Magnetization curves $M(B)$ of 2D nanostructures of magnetic particles as a function of applied magnetic field B. Results are given for weak (solid) and large (dotted) particle-size dispersion.

5 Conclusion

Several remarkable properties of two-dimensional ensembles of interacting magnetic nanoparticles have been identified. The complex noncollinear nature of the low temperature magnetic configurations which stability increases with disorder, the unusual scaling behavior of the magnetic energy as a function of particle concentration, the possibility of long range magnetic order due to dipolar interactions, or the complexity of the hysteresis loops are some examples. Further investigations are certainly needed in order to explore thoroughly the role of the different sample parameters and in order to shed light on other related effects, such as the relaxation dynamics under an external magnetic field, or the presence of spin-glass transitions.

Work financed in part by the EU GROWTH project AMMARE (G5RD-CT-2001-00478). Computer resources were provided by IDRIS (France). One of the authors (PJJ) acknowledges support from CNRS (France).

References

1. For a review see J.L. Dormann *et al.*, Adv. Chem. Phys. **98**, 283 (1997).
2. S. Sun *et al.*, Science **287**, 1989 (2000); M. Giersig and M. Hilgersdorff, J. Phys. A **32**, L111 (1999); M. Respaud *et al.*, Phys. Rev. B **57**, 2925 (1998); V. Russier *et al.*, *ibid.* **62**, 3910 (2000).
3. T. Jonsson *et al.*, Phys. Rev. Lett. **81**, 3976 (1998); C. Djurberg *et al.*, *ibid.* **79**, 5154 (1997); H. Mamiya *et al.*, *ibid.* **82**, 4332 (1999); P. Jönsson *et al.*, Phys. Rev. B **61**, 1261 (2000); M. Garcia del Muro *et al.*, *ibid.* **59**, 13 584 (1999); Jinlong Zhang *et al.*, Phys. Rev. Lett. **77**, 390 (1996).
4. R.W. Chantrell *et al.*, J. Magn. Magn. Mater. **157/158**, 250 (1996); J.J. Weis and D. Levesque, Phys. Rev. Lett. **71**, 2729 (1993); M.A. Załuska-Kotur, Phys. Rev. B **54**, 1064 (1996). D. Kechrakos and K.N. Trohidou, *ibid.* **58**, 12 169 (1998).
5. K. Binder and A.P. Young, Rev. Mod. Phys. **58**, 801 (1986).
6. K. De'Bell *et al.*, Phys. Rev. B **55**, 15 108 (1997); A. M. Abu-Labdeh *et al.*, *ibid.* **65**, 024434 (2001); A. Carbognani *et al.*, *ibid.* **62**, 1015 (2000).
7. J. Villain, Z. Phys. B **33**, 31 (1979); C.L. Henley, Phys. Rev. Lett. **62**, 2056 (1989); S. Prakash and C.L. Henley, Phys. Rev. B **42**, 6574 (1990).
8. U. Bovensiepen *et al.*, J. Magn. Magn. Mater. **192**, L386 (1999).
9. P.J. Jensen, Ann. Physik **6**, 317 (1997).
10. R. H. Swendsen and J.-S. Wang, Phys. Rev. Lett. **57**, 2607 (1986).
11. C.J. Geyer, in *Computing Science and Statistics: Proceedings of the 23rd Symposium on the Interface*, Americal Statistical Association (New York, 1991), p. 156.
12. F. Wang and D. P. Landau, Phys. Rev. Lett. **86**, 2050 (2001); Phys. Rev. E **64**, 056101 (2001).